

Precision Measurements Of Heavy Objects Working Group Summary

Marcel Demarteau,^a Vassilis Koulovassilopoulos,^b Joseph Lykken,^a Fredrick I. Olness,^{c†}
Stephen Parke,^{a*} Randall J. Scalise,^{c†} Erich Varnes,^d and G. P. Yeh,^{a*}

^a *Fermi National Accelerator Laboratory, Batavia, IL 60510 USA*

^b *Universitat de Barcelona, Dept. E.C.M., Facultat de Fisica, Diagonal 647, 08028 Barcelona, SPAIN*

^c *Southern Methodist University, Department of Physics, Dallas, TX 75275-0175 USA*

^d *Lawrence Berkeley National Laboratory, Berkeley, CA 94720 USA*

ABSTRACT

We report on the activities of the Precision Measurements Of Heavy Objects working group of the Very Large Hadron Collider Physics and Detector Workshop.

I. INTRODUCTION

The topics discussed by the Precision Measurements Of Heavy Objects working group spanned a very wide range; consequently, it is impossible to cover each topic in depth. Therefore, in this report we will primarily focus on the issues most relevant to a VLHC machine. In the following, we mention only the highlights, and refer the reader to the literature for more specific questions.

II. PARTON DISTRIBUTIONS FOR VLHC¹

Global QCD analysis of lepton-hadron and hadron-hadron processes has made steady progress in testing the consistency of perturbative QCD (pQCD) within many different sets of data, and in yielding increasingly detailed information on the universal parton distributions.²

We present the kinematic ranges covered by selected facilities relevant for the determination of the universal parton distributions. While we would of course like to probe the full $\{x, Q\}$ space, the small x region is of special interest. For example, the rapid rise of the F_2 structure function observed at HERA suggests that we may reach the parton density saturation region more quickly than anticipated. Additionally, the small x region can serve as a useful testing ground for BFKL, diffractive phenomena, and similar processes. Conversely, the production of new and exotic phenomena generally happens in the region of relatively high x and Q .

This compilation provides a useful guide to the planning of future experiments and to the design of strategies for global analyses. Another presentation regarding future and near-future machines is given in the 1996 Snowmass Structure Functions Working Group report.[1]

Here we will simply mention a few features which are particularly relevant for such a very high energy facility as a VLHC.

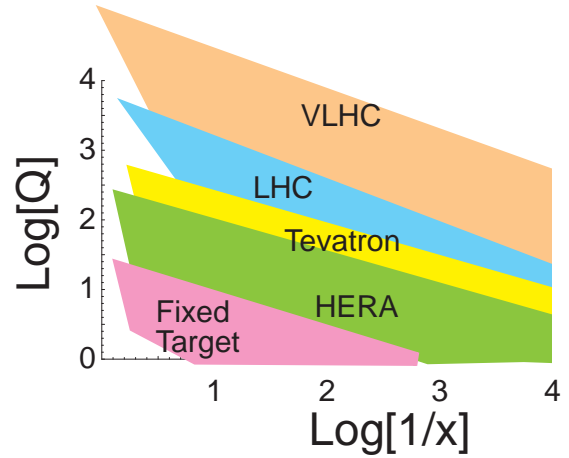


Figure 1: Kinematic range of various machines. Note the small x range is clipped in this plot. The Q scale is in GeV and the logs are base 10.

As we see in Fig. 1, the VLHC will probe an $\{x, Q\}$ region far beyond the range of present data. To accurately calculate processes at a VLHC, we must have precise PDF's in this complete kinematic range. Determining the PDF's in the small x regime is a serious problem since there will be no other measurement in the extreme kinematic domain required by VLHC. For the large x and Q region, the PDF's at large Q can, in principle, be determined via the standard QCD DGLAP evolution, but in practice uncertainties from the small x region can contaminate this region.

In Fig. 2, we display the evolution of the PDF's for a selection of partons. For the gluon and the valence quarks, we see a decrease at high x and an increase at low x with $x \sim 0.1$ as the crossing point. In contrast, for the heavy quark PDF's, we see generally an increase with increasing Q . The momentum fraction of the partons vs. energy scale is shown in Table I. An interesting feature to note here is the approximate "flavor democracy" at large energy scales; that is, as we probe the proton at very high energies, the influence of the quark masses becomes smaller, and all the partonic degrees of freedom carry comparable momentum fractions. To be more precise, we see

* Convenor, [†] sub-group report editor. Work supported in part by NSF and DOE.

¹Based on the presentation by Fredrick Olness.

²PDF sets are available via WWW on the CTEQ page at <http://www.phys.psu.edu/~cteq/> and on the The Durham/RAL HEP Database at <http://durpdg.dur.ac.uk/HEPDATA/HEPDATA.html>.

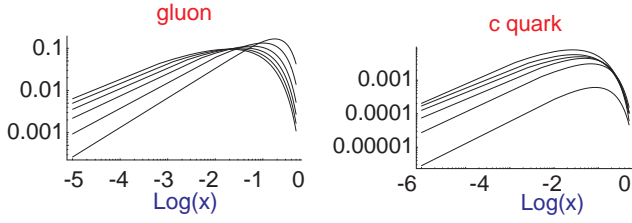


Figure 2: Evolution of the a) gluon and b) charm PDF's in Q vs. x . We display $x^2 f_{i/P}(x, Q)$ for $Q = \{2, 10^1, 10^2, 10^3, 10^4, 10^5\}$ GeV.

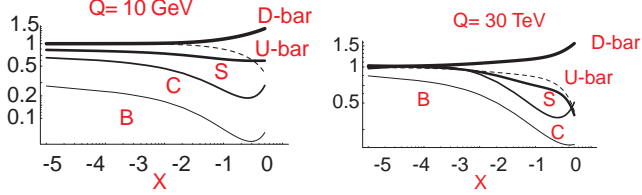


Figure 3: Flavor democracy at a) 10 GeV and b) 30 TeV. We compare the individual parton distributions $f_{i/P}(x, Q)$ to that of the average sea, $(\bar{u} + \bar{d})/2$.

that at the very highest energy scales relevant for the VLHC, the strange and charm quark are on par with the up and down sea, (while the bottom quark lags behind a bit). This feature is also displayed in Fig. 3 where we show these contributions for two separate scales. In light of this observation, we must dispense with preconceived notions of what are “traditionally” heavy and light quarks, and be prepared to deal with all quark on an equal footing at a VLHC facility. This approach is discussed in the following section.

Table I: Momentum fraction (in percent) carried by separate partons as a function of the energy scale Q .

Q	g	\bar{u}	\bar{d}	s	c	b
3 GeV	46	5	7	3	1	0
10 GeV	48	6	8	4	2	0
30 GeV	48	6	8	5	3	1
100 GeV	48	7	8	5	3	2
300 GeV	49	7	8	6	4	2
1 TeV	49	7	8	6	4	3
3 TeV	49	7	8	6	4	3
10 TeV	50	7	9	6	5	4
30 TeV	50	7	9	7	6	4
100 TeV	51	7	10	7	7	4

III. HEAVY QUARK HADROPRODUCTION³

Improved experimental measurements of heavy quark hadroproduction has increased the demand on the theoretical community for more precise predictions.[2, 3, 4, 5, 6] The first Next-to-Leading-Order (NLO) calculations of charm and bottom hadroproduction cross sections were performed some years ago.[3] As the accuracy of the data increased, the theoretical predictions displayed some shortcomings: 1) the theoretical cross-sections fell well short of the measured values, and 2) they displayed a strong dependence on the unphysical renormalization scale μ . Both these difficulties indicated that these predictions were missing important physics.

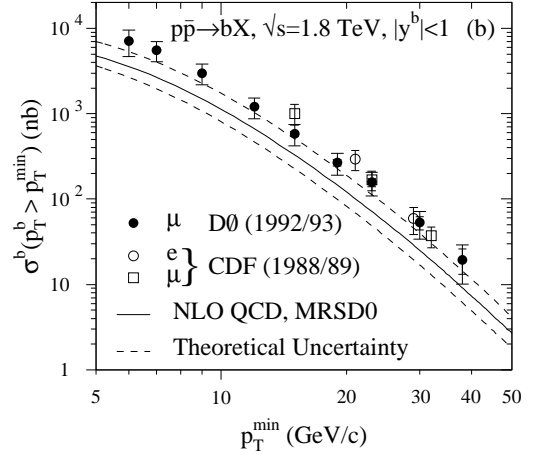


Figure 4: Heavy quark hadroproduction data. Cf., Ref. [2].

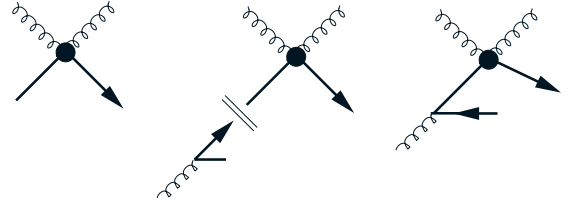


Figure 5: a) Generic leading-order diagram for heavy-flavor excitation (LO-HE), $gQ \rightarrow gQ$. b) Subtraction diagram for heavy-flavor excitation (SUB-HE), $^1 f_{g \rightarrow Q} \otimes \sigma(gQ \rightarrow gQ)$. c) Next-to-leading-order diagram for heavy-flavor creation (NLO-FC).

These deficiencies can, in part, be traced to large contributions generated by logarithms associated with the heavy quark mass scale, such as⁴ $\ln(s/m_Q^2)$ and $\ln(p_T^2/m_Q^2)$. Pushing the calculation to one more order, formidable as it is, would not

³Based on the presentation by Randall J. Scalise.

⁴Here, m_Q is the heavy quark mass, s is the energy squared, and p_T is the transverse momentum.

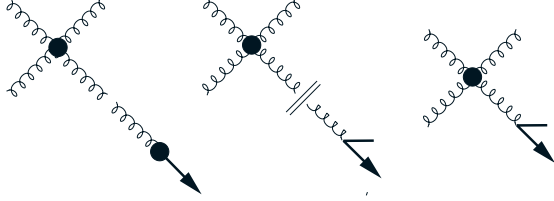


Figure 6: a) Generic leading-order diagram for heavy-flavor fragmentation (LO-HF), $\sigma(gg \rightarrow gg) \otimes D_{g \rightarrow Q}$. b) Subtraction diagram for heavy-flavor fragmentation (SUB-HF), $\sigma(gg \rightarrow gg) \otimes {}^1d_{g \rightarrow Q}$. c) Next-to-leading-order diagram for heavy-flavor creation (NLO-FC).

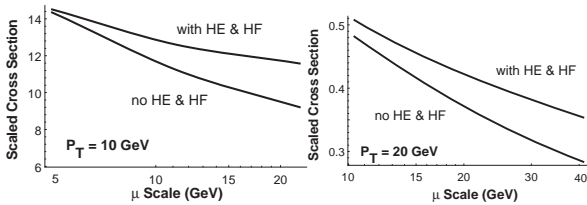


Figure 7: The scaled differential cross section $p_T^5 d^2 \sigma / dp_T^2 dy$ at $p_T = 10, 20 \text{ GeV}$ and $y = 0$ in $(pb - \text{GeV}^3)$ vs. μ . The lower curves (thin line) are the heavy quark production cross sections *ignoring* heavy-flavor excitation (HE) and heavy-flavor fragmentation (HF). The upper curves (thick line) are the heavy quark production cross sections *including* HE and HF. Cf., Ref. [6].

necessarily improve the situation since these large logarithms persist to every order of perturbation theory. Therefore, a new approach was required to include these logs.

In 1994, Cacciari and Greco[5] observed that since the heavy quark mass played a limited dynamical role in the high p_t region, one could instead use the massless NLO jet calculation convoluted with a fragmentation into a massive heavy quark pair to compute more accurately the production cross section in the region $p_t \gg m_Q$. In particular, they find that the dependence on the renormalization scale is significantly reduced.

A recent study[6] investigated using initial-state heavy quark PDF's and final-state fragmentation functions to resum the large logarithms of the quark mass. The principle ingredient was to include the leading-order heavy-flavor excitation (LO-HE) graph (Fig. 5) and the leading-order heavy-flavor fragmentation (LO-HF) graph (Fig. 6) in the traditional NLO heavy quark calculation.[3] These contributions can not be added naively to the $\mathcal{O}(\alpha_s^3)$ calculation as they would double-count contributions already included in the NLO terms; therefore, a subtraction term must be included to eliminate the region of phase space where these two contributions overlap. This subtraction term plays the dual role of eliminating the large unphysical collinear logs in the high energy region, and minimizing the renormalization scale dependence in the threshold region. The complete calculation including the contribution of the heavy quark PDF's and fragmentation functions 1) increases the theoretical prediction, thus moving it closer to the experimental data, and 2) reduces the μ -dependence of the full calculation, thus improving the predictive power of the theory. (Cf., Fig 7.)

In summary, the wealth of data on heavy quark hadroproduction will allow for precise tests of many different aspects of the theory, namely radiative corrections, resummation of logs, and multi-scale problems. Resummation of the large logs associated with the mass is an essential step necessary to bring theory in agreement with current experiments and to make predictions for the VLHC.

IV. W MASS STUDIES⁵

The W boson mass is one of the fundamental parameters of the standard model; its precision measurement can be used in conjunction with the top mass to extract information on the Higgs boson mass. The W boson mass has already been measured precisely, and the current world average is: $M_W = 80.356 \pm 0.125 \text{ GeV}/c^2$.

Here, we focus on issues which are unique to a VLHC facility, and refer the reader to the literature for details regarding other topics.[7, 8, 9, 10] The question addressed in the working group session was to consider the expected precision for M_W at the VLHC in comparison to what will be available from competing facilities at VLHC turn-on. For our estimates, we use $\sqrt{s} = 100 \text{ TeV}$, $\Delta t = 16.7 \text{ ns}$ (the bunch spacing), $\sigma_{tot} \simeq 120 \text{ mb}$, and 20 interactions per crossing.

For W events produced in a hadron collider environment there are essentially only two observables that can be measured: i) the

⁵Based on the presentation by Marcel Demarteau.

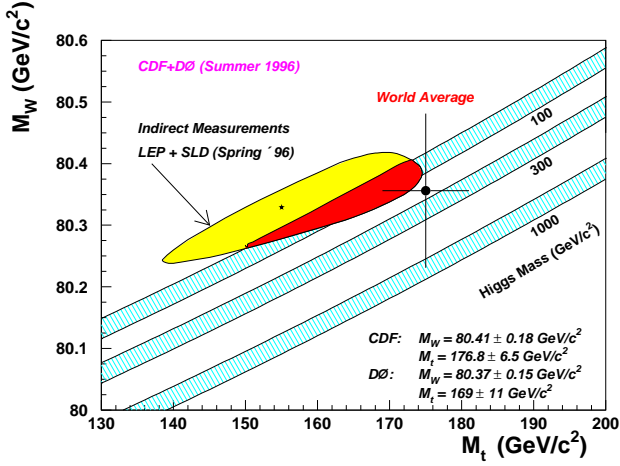


Figure 8: Plot of M_W vs. M_t with DØ and CDF preliminary measurements of the W boson and top quark masses. Bands indicate the Standard Model constraints for different Higgs mass values. Indirect measurements from LEP I are also shown. (June, 1997) Taken from Ref. [9].

lepton momentum, and *ii*) the transverse momentum of the recoil system. The transverse momentum of the neutrino must be inferred from these two observables. The W boson mass can be extracted from either the lepton transverse momentum distribution, or the transverse mass: $M_T = \sqrt{2p_T^e p_T^\nu (1 - \cos \phi^{e\nu})}$, where $\phi^{e\nu}$ is the angle between the electron and neutrino in the transverse plane.

It is important to note that the following estimates necessitate a large extrapolation from $\sqrt{s} = 1.8$ TeV to $\sqrt{s} = 100$ TeV. For the W decays, the observed number distribution in pseudorapidity (η) can be estimated by scaling results from the CERN $S\bar{p}pS$ and the Fermilab Tevatron. The shoulder of the pseudorapidity plateau is ~ 3 for $\sqrt{s} = 630$ GeV, and ~ 4 for $\sqrt{s} = 1.8$ TeV. This yields an estimate in the range of ~ 5 to 9 for a $\sqrt{s} = 100$ TeV VLHC. Assuming coverage out to $|\eta| \leq 4$, we obtain ~ 1400 charged tracks in the detector calorimeter with which we must contend for the missing E_T calculation, (\cancel{E}). Scaling the $\langle p_T \rangle$ up to $\sqrt{s} = 100$ TeV we estimate $\langle p_T \rangle \simeq 865$ MeV for minimum bias tracks. Assuming $N_{ch}/N_\gamma = 1$ yields an average E_T flow of 2 TeV in the detector. Using current \cancel{E}_T resolutions of $\sim 4 - 5$ GeV, we estimate $\sigma(\cancel{E}_T) \simeq 25 - 30$ GeV for VLHC.

Two fundamental problems we encounter at a VLHC are multiple interactions and pile-up. Multiple interactions are produced in the same crossing as the event triggered on. The effects are “instantaneous;” *i.e.*, the electronic signals are added to the trigger signals and subjected to the same electronics. Pile-up effects are out-of-time signals from interactions in past and future buckets caused by “memory” of the electronics. Both cause a bias and affect the resolution, but in different ways. The effect of pile-up is strongly dependent on the electronics used in relation to the bunch spacing.

The bottom line is the estimation of the total uncertainty on

the W mass, δM_W . For a luminosity of 2 fb^{-1} , δM_W is about 20 MeV for both the transverse mass and lepton transverse momentum fits. For an increased luminosity of 10 fb^{-1} , the transverse mass fit might improve to $\delta M_W \sim 15 \text{ MeV}$, with minimal improvement for the determination from the lepton transverse momentum distribution. It should be noted that these estimates have quite a few caveats—additional study would be required before taking these numbers as guaranteed predictions. In Table II, we compare these estimations with the anticipated uncertainty from upcoming experiments. Clearly the VLHC will not greatly improve the determination of M_W . The situation becomes more difficult when one insists that the VLHC detectors be capable of *precisely* measuring the relatively low energy leptons from the M_W decay.

Table II: Anticipated limits on δM_W from present and future facilities. (This compilation is taken from Ref. [9].)

FACILITY	$\delta M_W \text{ (MeV/c}^2\text{)}$	\mathcal{L}
NuTeV	~ 100	—
HERA	~ 60	150 pb^{-1}
LEP2	$\sim 35\text{-}45$	500 pb^{-1}
Tevatron	~ 55	1 fb^{-1}
Tevatron	~ 18	10 fb^{-1}
LHC	$\lesssim 15$	10 fb^{-1}
VLHC	~ 20	1 fb^{-1}
VLHC	~ 15	10 fb^{-1}

V. THE TOP QUARK⁶

The mass of the recently discovered top quark is precisely determined by the CDF and DØ collaborations from $t\bar{t}$ production at the Tevatron. For the details of this discovery and measurement, we refer the reader to Refs. [11, 12, 13, 14].

In Table III, we display the anticipated accuracy on the top quark mass at the Tevatron as estimated in the TeV2000 report.[15] Since this report, statistical techniques have been improved such that one would expect a precision of $\delta m_t \sim 1.5$ GeV with 10 fb^{-1} , assuming other sources of systematics are negligible.

Moving on to the LHC, the top production cross section is ~ 100 times greater than at TeV2000, so with a luminosity of $\sim 100 \text{ fb}^{-1}/\text{year}$, we expect ~ 1000 more top events after one LHC year. Assuming naively that the errors scale as $1/\sqrt{N}$ (where N is the number of events), we would obtain $\delta m_t \sim 50$ MeV.

The challenges of the VLHC are quite similar to the LHC regarding this measurement. A precision measurement of the top quark mass at this level (or better) places stringent demands on the jet calibration. Even with large control samples of $Z + \text{jets}$ and $\gamma + \text{jets}$, uncertainties due to the ambiguous nature of jet definitions will persist. The large number of multiple interactions at LHC and VLHC complicates this analysis (in a manner

⁶Based on the presentation by Erich Varnes.

similar to that discussed for the W boson mass measurement). Therefore, in order to improve upon existing measurements, the VLHC detectors will need to be extremely well designed and understood—certainly a heroic task.

Table III: Anticipated accuracy on the top quark mass, as estimated by the TeV2000 report.[15]

Source	70 pb^{-1}	1 fb^{-1}	10 fb^{-1}
Statistics	25	6.2	2
Jet Scale	11	2.7	0.9
Backgrounds	4	1	0.3
Total	27.6	6.9	2.2

VI. PROBING A NONSTANDARD HIGGS BOSON AT A VLHC⁷

We have studied the potential of a VLHC to observe a non-standard Higgs boson (i.e. a spin-0 isospin-0 particle with nonstandard couplings to weak gauge bosons and possibly fermions) and distinguish it from the Standard Model Higgs boson. Results are presented for different options for the energy ($\sqrt{s} = 50, 100, 200 \text{ TeV}$) and luminosity ($\mathcal{L} = 10^{33} - 10^{35} \text{ cm}^{-2} \text{ s}^{-1}$) and compared to those obtained for the LHC in Ref. [16].

Our analysis is based on the gold-plated channel $H \rightarrow ZZ \rightarrow l^+l^-l^+l^-$ and assumes cuts on the final-state leptons, which are given by $|\eta^l| < 3$, $p_T^l > 0.5 \times 10^{-3} \sqrt{s}$. We studied Higgs masses in the range from 400 to 800 GeV (600-800 GeV for $\sqrt{s} = 200 \text{ TeV}$), where the lower limit is due to the cuts and the upper limit is theoretically motivated.

The two relevant parameters that encode the deviations from the Standard Model (SM) are ξ and y_t , the $HW^+W^-(HZZ)$ and $Ht\bar{t}$ couplings relative to the SM respectively. We found that a nonstandard Higgs should be detected for practically all values of ξ , y_t and \mathcal{L} in the entire mass range studied, a situation which is not so clear for the LHC, particularly for the larger masses.

A nonstandard Higgs boson can be distinguished from the SM one by a comparison of its width Γ_H and the total cross-section. Due to theoretical uncertainties in the latter, we chose to use as a criterion only the measurement of the width. Following the procedure of ref. [16] we quantified the statistical significance of a deviation from the SM prediction by constructing the probability density function according to which the possible measurements of the *Standard Model* width are distributed. Postulating that a nonstandard Higgs boson is “distinguishable” if its width differs from the SM value by at least 3σ , we were able to determine the precision with which the parameter ξ can be measured at the LHC and a VLHC. This is summarized in Table VI for the case of $y_t = 1$. We deduce that, for the purpose of precision measurements of the Higgs couplings, a lower energy VLHC with higher luminosity is preferred to that of a

Table IV: Approximate sensitivity to the parameter ξ at the LHC and the VLHC for various values of the luminosity and CM energy. The starred entries indicate that the value given applies only to $\xi > 1$, whereas for $\xi < 1$ the sensitivity is substantially worse.

$\sqrt{s}, \mathcal{L} \text{ (cm}^{-2} \text{ s}^{-1}\text{)}$	Sensitivity to ξ		
	$m_H = 400 \text{ GeV}$	600 GeV	800 GeV
14 TeV, 10^{33}	60% *	—	—
14 TeV, 10^{34}	20% *	40% *	—
50 TeV, 10^{34}	7%	12%	20%
50 TeV, 10^{35}	3%	4%	7%
100 TeV, 10^{34}	6%	8%	12%
100 TeV, 10^{35}	2-3%	3%	5%
200 TeV, 10^{33}	—	25%	30%
200 TeV, 10^{34}	—	8%	12%

higher energy with lower luminosity — a conclusion that is due to the low-mass character of the physics of interest.

Consequently, we find that for Higgs masses in the range from 400 to 800 GeV, the Higgs-Z-Z coupling can be measured to within a few percent at the VLHC, depending on the precise mass and collider parameters.

VII. SUPERSYMMETRY⁸

Supersymmetry (SUSY) is a dominant framework for formulating physics beyond the standard model in part due to the appealing phenomenological and theoretical features. SUSY is the only possible extension of the spacetime symmetries of particle physics, SUSY easily admits a massless spin-2 (graviton) field into the theory, and SUSY appears to be a fundamental ingredient of superstring theory. Given the large number of excellent recent reviews and reports on SUSY,[17, 18, 19] we will focus here on the issues directly related to the VLHC.

One specific question which was addressed in the working group meeting was: Is the VLHC a precision machine for standard weak-scale SUSY with sparticle masses in the range 80 GeV to 1 TeV? Probably not, for the following reasons.

- An order of magnitude increase in sparticle production rates will yield minimal gains, *except* for sparticles in the range $\gtrsim 1 \text{ TeV}$.
- Multiple interactions, degraded tracking, calibration, and b-tagging issues complicate reconstruction of the SUSY decay chains.

On the contrary, VLHC looks best if SUSY has some heavy surprises in store such as $\gtrsim 1 \text{ TeV}$ squarks, or $\sim 10 \text{ TeV}$ SUSY messengers.

One example of a plausible SUSY scenario would be heavy first and second generation squarks and sleptons (to suppress FCNC's) with a characteristic mass in the range of $\sim 3 \text{ TeV}$.

⁷Based on the presentation by Vassilis Koulovassilopoulos.

⁸Based on the presentation by Joseph Lykken.

(Cf., Ref. [19]) While the gauginos and the third generation squarks and sleptons would be within reach of the LHC, investigation of $\{\tilde{u}, \tilde{d}, \tilde{e}, \tilde{\nu}_e\}$ and $\{\tilde{c}, \tilde{s}, \tilde{\mu}, \tilde{\nu}_\mu\}$ in the multi-TeV energy range would require a higher energy facility such as the VLHC.

An estimate of the heavy squark signal over the weak-scale SUSY background and conventional channels (such as $t\bar{t}$) indicates that a VLHC can observe heavy quarks in the ~ 3 TeV mass range; such a heavy squark is difficult to reach at the LHC. One might expect on order of $10^3 - 10^4$ signal events/year. Of course, background rejection is a serious outstanding question, and the efficiency of b-tagging and high p_t lepton rejection, for example, are crucial to suppressing the backgrounds.

VIII. CONCLUSIONS

While these individual topics are diverse, there are some common themes we can identify with respect to a VLHC machine. First, a very high energy hadron collider does not appear to be the machine of choice for precision measurements in the energy range $\lesssim 500$ GeV. The competition from Tevatron, HERA, LEP, and LHC are formidable in this region. To obtain comparable precision, the VLHC is handicapped by numerous factors including multiple interactions, large multiplicity, and large \cancel{E} . Designing a detector to operate in the VLHC environment while achieving the precision of the lower energy competition is a challenging task.

In contrast, the strong suit of the VLHC is clearly its kinematic reach. Should there be unexpected sparticles in the \gtrsim TeV range, the VLHC would prove useful in exploring this range. Of course our intuition as to what might exist in the ~ 10 TeV regime is not as refined as the $\lesssim 1$ TeV regime which will be explored in the near-future; however what we discover in this energy range can provide important clues as to where we should search with a VLHC.

IX. REFERENCES

- [1] 1996 Snowmass Structure Functions Working Group report, hep-ph/9706470. And references therein.
- [2] CDF Collaboration: V. Papadimitriou. FERMILAB-CONF-95-128-E. DØ Collaboration: L. Markosky. FERMILAB-CONF-95-137-E; Kamel A. Bazizi. FERMILAB-CONF-95-238-E.
- [3] P. Nason, ETH-PT/88-11. P. Nason, S. Dawson, R.K. Ellis, Nucl.Phys. **B327**, 49 (1989), Err.-ibid.B335, 260 (1990). ibid. **B303**, 607 (1988). M.L. Mangano, P. Nason, G. Ridolfi. ibid. **B405**, 507 (1993). W. Beenakker, H. Kuijf, W.L. van Neerven, J. Smith, Phys.Rev. **D40**, 54 (1989).
- [4] J. Collins, W. Tung., Nucl.Phys.**B278**, 934 (1986). F. Olness, W.-K. Tung, Nucl.Phys. **B308**, 813 (1988). M. Aivazis, F. Olness, W. Tung, Phys.Rev.Lett. 65, 2339 (1990). Phys.Rev. **D50**, 3085 (1994). M. Aivazis, J. Collins, F. Olness, W. Tung, Phys.Rev. **D50**, 3102 (1994).
- [5] M. Cacciari, M. Greco, Nucl.Phys.**B421**, 530 (1994). Z.Phys.**C69**, 459 (1996). B. Mele, P. Nason, Phys.Lett.**B245**, 635 (1990). Nucl.Phys.**B361**, 626 (1991).
- [6] F.I. Olness, R.J. Scalise, and W.-K. Tung, SMU-HEP-96/08; J.C. Collins, F.I. Olness, R.J. Scalise, and W.-K. Tung, CTEQ-616 (in preparation).
- [7] "Precision Electroweak Measurements," M. Demarteau, DPF, 1996, FERMILAB-Conf-96/354.
- [8] "Electroweak Results from the Tevatron," M. Demarteau, Snowmass, 1996, Fermilab-Conf-96/353.
- [9] "Precision Electroweak Physics at Future Collider Experiments," U. Baur and M. Demarteau, Talk given at 1996 DPF/DPB Summer Study on New Directions for High-energy Physics (Snowmass 96), Snowmass, CO, 25 Jun - 12 Jul 1996, FERMILAB-CONF-96-423, hep-ph/9611334.
- [10] "Future Electroweak Physics at the Fermilab Tevatron," Report of the TEV-2000 Study Group, (D. Amidei *et al.*), FERMILAB-PUB-96-082, Apr 1996.
- [11] CDF Collaboration, (F. Abe *et al.*), "Observation of Top Quark Production in Anti-p p Collisions," Phys. Rev. Lett. **74** 2626-2631, 1995.
- [12] DØ Collaboration, (S. Abachi *et al.*), "Observation of the Top Quark," Phys. Rev. Lett. **74** 2632 (1995).
- [13] DØ Collaboration, (S. Abachi *et al.*), "Direct Measurement of the Top Quark Mass," hep-ex/9703008.
- [14] DØ Collaboration, (B. Abbott *et al.*), "Measurement of the Top Quark Mass Using Dilepton Events," hep-ex/9706014.
- [15] D. Amidei and R. Brock, *eds.* Future ElectroWeak Physics at the Fermilab Tevatron: Report of the TeV2000 Study Group. FERMILAB-Pub-96/082
- [16] "The Profile Of A Nonstandard Higgs Boson At The LHC," Dimitris Kominis, Vassilis Koulovassilopoulos, Phys. Rev. **D52**, (1995), 2737.
- [17] "Introduction to Supersymmetry," J.D. Lykken, Talk given at Theoretical Advanced Study Institute in Elementary Particle Physics (TASI 96): Fields, Strings, and Duality, Boulder, CO, 2-28 Jun 1996, FERMILAB-PUB-96-445-T, hep-th/9612114.
- [18] "Report of the Supersymmetry Theory Subgroup," J. Amundson *et al.*, Report of the Snowmass Supersymmetry Theory Working Group, Sep 1996, hep-ph/9609374.
- [19] A. Bartl *et al.*, "Supersymmetry at LHC," Presented at 1996 DPF/DPB Summer Study on New Directions for High-Energy Physics (Snowmass 96), Snowmass, CO, 25 Jun - 12 Jul 1996. LBL-39413, Nov 1996.